aerospace

MDPI

Article

Superhydrophobic Coatings for Corrosion Protection of Stainless Steel

Filomena Piscitelli [1,*] and Annalisa Volpe [2,3]

[1] Italian Aerospace Research Centre, CIRA, Via Maiorise, 1, 81043 Capua, Italy
[2] Dipartimento Interateneo di Fisica, Politecnico di Bari, Via G. Amendola 173, 70125 Bari, Italy; annalisa.volpe@poliba.it
[3] CNR-IFN UOS BARI, Via Amendola 173, 70125 Bari, Italy
* Correspondence: f.piscitelli@cira.it

Abstract: Corrosion is a persistent challenge in the aviation industry, affecting the safety, performance, and maintenance costs of aircraft. While composite materials have gained widespread use due to their lightweight properties and corrosion resistance, certain critical parts, such as the wing and empennage leading edges and the engine inlet, demand alternative solutions. Aluminum, titanium, and stainless steel emerge as mandatory materials for such components, given their exceptional strength and durability. However, protecting these metallic components from corrosion remains crucial. In this paper, we present a study aimed at evaluating the corrosion resistance of stainless steel, employed as an erosion shielding panel for a composite vehicle's wing, layered with a superhydrophobic coating. The samples with and without coating have been characterized by contact angle measurements, microscopy (optical and electronic), and visual inspection after immersion in two solutions, NaCl and NaOH, respectively. The application of the superhydrophobic coating demonstrated a significant reduction in corrosion extent, especially in the demanding NaCl environment. This was evidenced by diminished formation of ripples and surface roughness, decreased iron oxide formation from oxidative processes, and a lower Surface Free Energy value in both liquid environments. Notably, the surface maintained its superhydrophobic properties even following an 8-day immersion in NaCl and NaOH solutions, demonstrating the reliability of the superhydrophobic coating offering as a potential solution to enhance the longevity and reliability of aircraft structures.

Keywords: superhydrophobic coating; corrosion; stainless steel; leading edge; aircraft; passive IPS

Citation: Piscitelli, F.; Volpe, A. Superhydrophobic Coatings for Corrosion Protection of Stainless Steel. *Aerospace* **2024**, *11*, 3. https://doi.org/10.3390/aerospace11010003

Academic Editor: Doni Daniel

Received: 21 November 2023
Revised: 6 December 2023
Accepted: 14 December 2023
Published: 19 December 2023

1. Introduction

The corrosion in aircraft structures, in particular aluminum, titanium, and steel alloys [1], is a persistent problem that directly impacts the performance, safety, and maintenance costs of aircraft [2,3]. To combat this issue, the aviation industry has explored various materials, among which composites have gained significant attention due to their lightweight nature. Composites offer excellent corrosion resistance, making them an attractive choice for many applications, including aircraft construction [4]. However, there are certain parts, such as the wing and empennage leading edges and the engine inlet, subject to impact, where composites may not be a suitable alternative due to specific design and structural requirements. While composite materials are generally strong and stiff, they can be more susceptible to impact damage compared to metals [4]. High-energy impacts, such as those from debris or bird strikes, can cause hidden internal damage or delamination that may compromise the structural integrity of the composite component. Moreover, while repairs are possible for composite structures, they can be more challenging than repairing metal structures. In fact, the repair process may require specialized equipment, materials, and expertise. In some cases, extensive damage to a composite component may necessitate its complete replacement rather than repair. In these cases, stainless steel, sometimes employed as an erosion shielding layer on composite substrate, emerges as a needed material

choice, given its high strength and superior mechanical properties that make it an ideal candidate for critical aircraft components particularly undergone to erosion from rain, sand, ice, and so on. However, to ensure its long-term performance, an engineering control of corrosion is essential. Raising awareness of the importance of corrosion protection, various methods are applied to corrosion control engineering, such as the development of novel corrosion-resistant materials, corrosion inhibitors, electrochemical cathodic protection and surface modifications, as well as coating [5,6]. Among these methods, coating is a simple and effective way for corrosion protection at a low cost.

Superhydrophobic coatings have gained attention in recent years for their remarkable water-repellent properties [7,8] and potential for protecting various surfaces from corrosion [9,10]. Hydrophobic and superhydrophobic coatings are a class of coatings that take advantage of the ability of the coating to repel water, moisture, and other aqueous solutions [11] by increasing nanoscale roughness and lowering surface tension [12]. Various methods are available for the nanofabrication of superhydrophobic coatings, depending on the type of functionalization and morphological modifications performed [13,14]. The superhydrophobic coatings that are relatively more common and have current significance are silane-modified superhydrophobic coatings [15], polymer-based coatings, coatings developed by soft lithography method, titanium oxide-based superhydrophobic coatings, and nanoparticle-based coatings that are repellent to numerous fluids [16]. In all cases, the corrosion resistance mechanism of superhydrophobic surfaces can be summarized as follows: when a superhydrophobic surface is immersed into a corrosive medium, an air layer is formed within the superhydrophobic surface and the liquid phase [17]. As widely demonstrated by electrochemical impedance spectroscopy (EIS), the retained air hindered the electron transfer between the metal and solution, resulting in effective corrosion protection for engineering materials [6].

Additionally, as widely reported [18–21], the water repellency of the superhydrophobic coatings slows down the transport of water containing corrosive ions to the underlying substrate, preserving its structural integrity. Li et al. demonstrated the feasibility of reducing the Zn corrosion rate to about one-eighth, changing the surface character from superhydrophilicity to superhydrophobicity by the use of a low-surface-energy compound. This notable improvement in corrosion resistance can be attributed to the obstructive and capillary effects induced by the superhydrophobic surface [22]. Superhydrophobic silica films deposited onto mild steel substrates have also been demonstrated to provide an effective barrier coating for the mild steel interface [23]. Liu et al. demonstrated that electrodeposition coatings provided greater protection against corrosion behavior in the case of copper substrates [24]. Similar results have been found applying superhydrophobic films based on low-surface-energy compounds on titanium [25]. The films showed higher corrosion resistance properties when immersed in a 3.5 wt.% NaCl aqueous solution for 90 days, as compared to modified titanium substrate, which indicated that the superhydrophobic films have a long-term corrosion resistance endurance. An investigation of the corrosion behavior of carbon steel coated with fluoropolymer thin films has also been performed, finding that the film is an interesting protective layer of metal and metal oxides [26].

It is noteworthy that in the aeronautical field, the aircraft parts particularly exposed to erosion are equally exposed to the ice formation; therefore, the water repellency of the superhydrophobic coatings with the double effect to reduce and delay the ice accretion and contemporary to protect the metallic substrate from corrosion have significant technological value. Consequently, delving into the corrosion resistance of coatings expressly designed for aerospace applications becomes an intriguing avenue for study.

The focus of this paper is to explore the corrosion behavior of stainless steel, employed as an erosion shielding panel for composite vehicle's wings, covered utilizing an innovative superhydrophobic coating specifically designed for aircraft construction. The experimental methodology employed in our study involves subjecting the coated stainless-steel samples to corrosion tests based on immersion in two aqueous solutions, NaCl and NaOH, respectively. The coated specimens before and after immersion are characterized through

visual inspection, optical and field emission scanning electron (SEM) microscopy, roughness, contact angle and Surface Free Energy (SFE) measurements, and surface elemental analysis by means of energy-dispersive X-ray spectroscopy. Results are compared to the corresponding references.

2. Materials and Methods

Flat tin-coated stainless-steel sheets (682-444 RS Components) 2 mm thick were used as a substrate for the experiments. The samples were sand abraded at 3 bar to increase roughness and improve the coating adhesion and cut into small samples of about 5×5 cm^2 for the reference and about 10×10 cm^2 for the coated samples. Then, the samples' surfaces were cleaned with polyester cellulose wipes embedded first with Metaflex and then with bi-distillated water, and then dried with compressed air. This cleaning step was repeated until the wipe appeared clean. After that, the surface was cleaned with isopropyl alcohol, then with ethyl alcohol, and finally dried with compressed air. Then, a nanostructured superhydrophobic coating (SHC), which formulation is reported in [27,28], was applied on the sample surface, as a usual paint, with an aerograph following a layer-by-layer process [29]. The SHC was applied after samples were cut in order to protect the samples' edges as well as their surface.

The solution immersion test [30–32] was performed on reference (R) and coated (C) samples at room temperature in two distinct aqueous solutions: (1) 5 wt.% NaCl (sodium chloride) in water at pH = 5.5 and (2) 0.1M NaOH (sodium hydroxide) at pH 13.

The samples were fully immersed in the solutions and left in immersion for 8 days without agitation or refreshing.

After 8 days in solution, each sample was cleaned by rubbing it gently with a soft dry tissue, then dried at 90 °C in an oven. The tests were conducted on a single specimen for each type of sample and immersion in solution.

The roughness of substrates was measured by employing a SAMA SA6260 surface roughness meter according to ISO 4288 [33]. The roughness measurements, reported as Ra, represent the arithmetic average of the absolute values of the profile height deviations from the mean line.

The optical images were acquired with a microscope USB Dino-Lite AM4815ZTL at 140×.

The contact angle (CA) measurements on the surfaces were performed at 23 °C in compliance with the ASTM D7490-13 standard [34], with 3µL of water (H_2O), diiodomethane (CH_2I_2), and formamide ($HCONH_2$). Contact angles were rapidly acquired within 30 s of depositing the drop to avoid changes in angles. At least 6 measurements were acquired, and average values and standard deviations were reported for each sample. The Surface Free Energy (SFE) was calculated according to the Owens Wendt (OW) method, for which the surface energy of a solid is the sum of two components, a dispersive and a polar one [35,36]:

$$\gamma_s = \gamma_s^p + \gamma_s^d \tag{1}$$

whereas the Work of Adhesion (WA) and Surface Polarity (SP) can be calculated as follows:

$$W_A = 2\left(\gamma_s^p \gamma_l^p\right)^{1/2} + 2\left(\gamma_s^d \gamma_l^d\right)^{1/2} \tag{2}$$

and

$$SP = \frac{\gamma^p}{\gamma^p + \gamma^d} \tag{3}$$

where γ_l^d, γ_l^p are the SFE components of the reference liquids. All details about the employed tool and method are described in [37].

The surface morphology of stainless-steel samples before and after immersion in solutions was examined by a Zeiss (Mod Sigma, Steinheim, Germany) field emission scanning electron microscope (SEM). The elemental mapping of the upmost layers, particularly the

corroded layers, was obtained using attached energy-dispersive X-ray spectroscopy (EDX). At least 3 measurements were acquired, and average values and standard deviations were reported for each sample.

3. Results

Figure 1a–f show the pictures of the reference (smaller) and coated (larger) stainless-steel samples before and after 8 days of immersion in NaCl and NaOH. A third sample with intermediate dimensions and painted with the coating's primer appears in Figure 1. Results are not discussed here because they are irrelevant to the scope of the present work. After 8 days, both NaCl and NaOH settled on the sample surface, creating a white spot (Figure 1). Then, the samples were re-immersed in distilled water (Figure 1e,f) in order to allow the salt crystals to dissolve again and to observe the samples' surfaces.

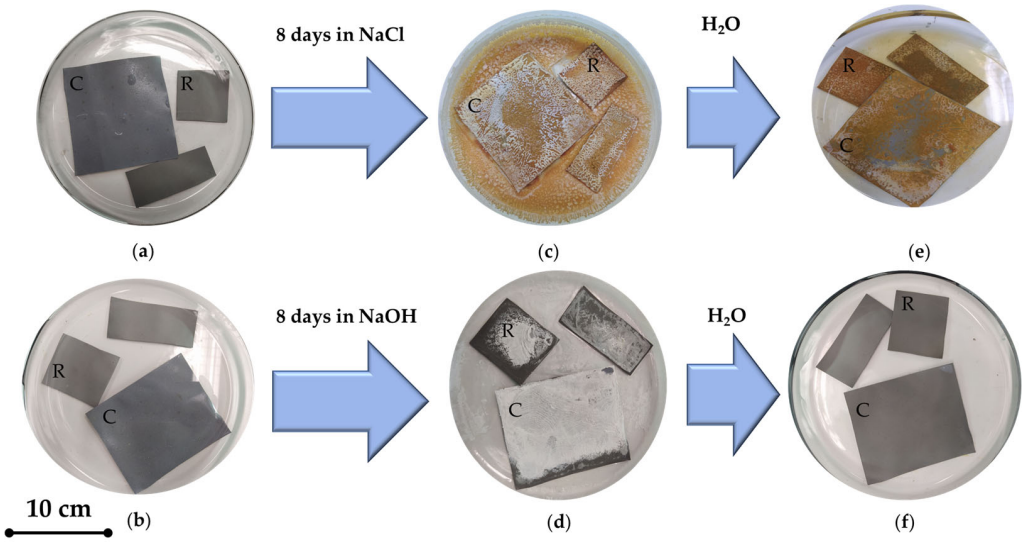

Figure 1. Pictures of the R and C samples just immersed in (**a**) NaCl and (**b**) NaOH; (**c**,**d**) samples after 8 days of immersion; and (**e**,**f**) after re-immersion in water.

At first glance, all the substrates subjected to the NaCl saline solution, in spite of the presence of the superhydrophobic coating, show more significant signs of corrosion than the sample subjected to the NaOH base. To further investigate the corrosion resistance of the samples in solution and the eventual role of the coating, further comparative tests have been conducted.

In Figure 2, the R sample, after immersion in NaCl (panel (a)) and after the subsequent cleaning and oven-drying (panel (b)) to remove the NaCl depositions, is presented. Due to the tendency of salt to precipitate on the metal surface, the formation of not uniform salt crystals can be clearly noticed. As also shown in Figure 3, the non-uniformity of salt distribution contributes to selective corrosion of the steel, as areas with high salt accumulation may be more prone to corrosion. The aggressiveness of the saline solution can be ascribed to various factors. First, salt is hygroscopic, meaning it absorbs water from the air. This makes it possible for corrosion to occur at lower relative humidity levels and for longer periods of time than otherwise expected. Second, salt increases water's ability to carry a current and speeds up the corrosion process [38]. Third, the chloride ions in salt can break down the protective oxide layer that forms on the surface of some metals, making the surface more vulnerable to corrosion [39]. Conversely, the presence of the superhydrophobic coating reduces the presence of salt crystals and the consequent corrosion of the sample, as shown in Figure 2c,d. Here, the corrosion appears as small spots distributed over the entire surface of the sample (Figure 3g–j). This effect can be ascribed to the reduction in the water contact area in the presence of the coating: the formation of air barriers over the superhydrophobic sample diminishes the interaction between such

metal surfaces and liquid, thus leading to better corrosion resistance and a lower corrosion rate [12].

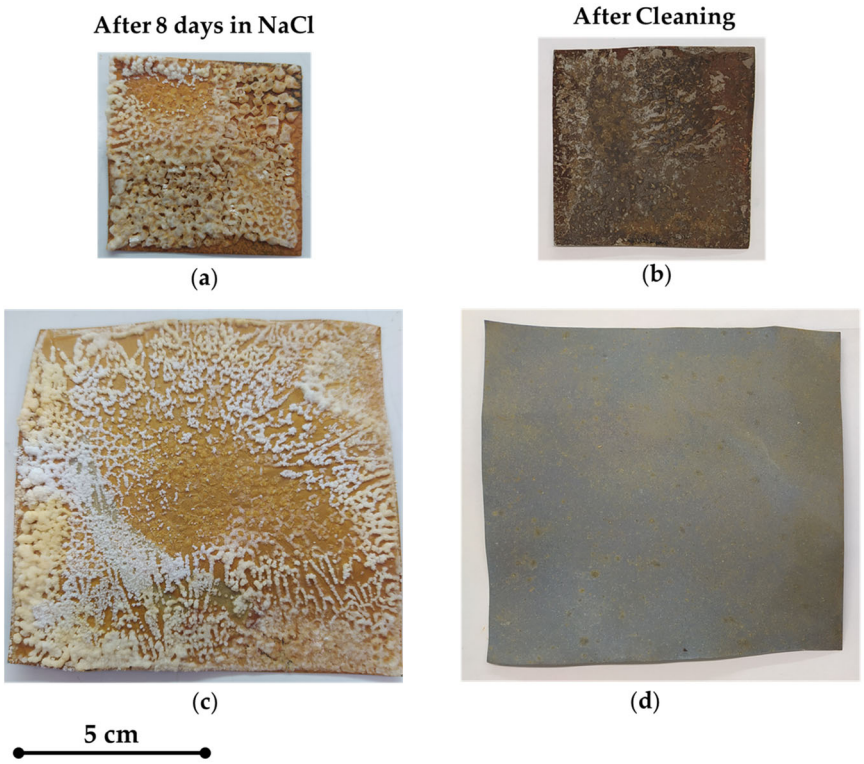

Figure 2. Pictures of the R sample after 8 days in NaCl (**a**) and after cleaning (**b**), and of the C sample after 8 days in NaCl (**c**) and after cleaning (**d**).

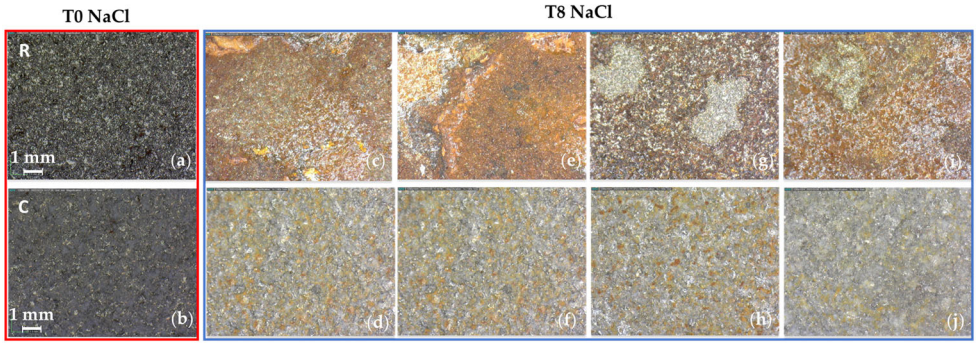

Figure 3. Microscopic image of the R sample (**a**) before and (**b**–**e**) after 8 days in NaCl and of the coated sample C (**f**) before and (**g**–**j**) after 8 days in the same solution.

In Figure 4, the R and C samples after 8 days in NaOH solution (panels (a) (c), respectively) and after subsequent cleaning and drying (panels (b) and (d)) are shown. Corrosion effects on the sample immersed in NaOH are less visible compared to those in NaCl, regardless of whether there is or is not a superhydrophobic coating, as confirmed by the optical images shown in Figure 5. Although less pronounced than in NaCl, immersion in NaOH solution may have a corrosive behavior of stainless steel in a process known as alkaline corrosion or hydroxide corrosion. During alkaline corrosion, hydroxide ions (OH^-) from the NaOH solution diffuse through the protective oxide film on the stainless steel. This leads to a local increase in pH on the metal surface, resulting in the formation of soluble iron hydroxides. This reaction leads to the dissolution of iron from the steel surface, whose

severity depends on factors such as the concentration of NaOH, temperature, exposure time, and the specific composition of the stainless steel [40].

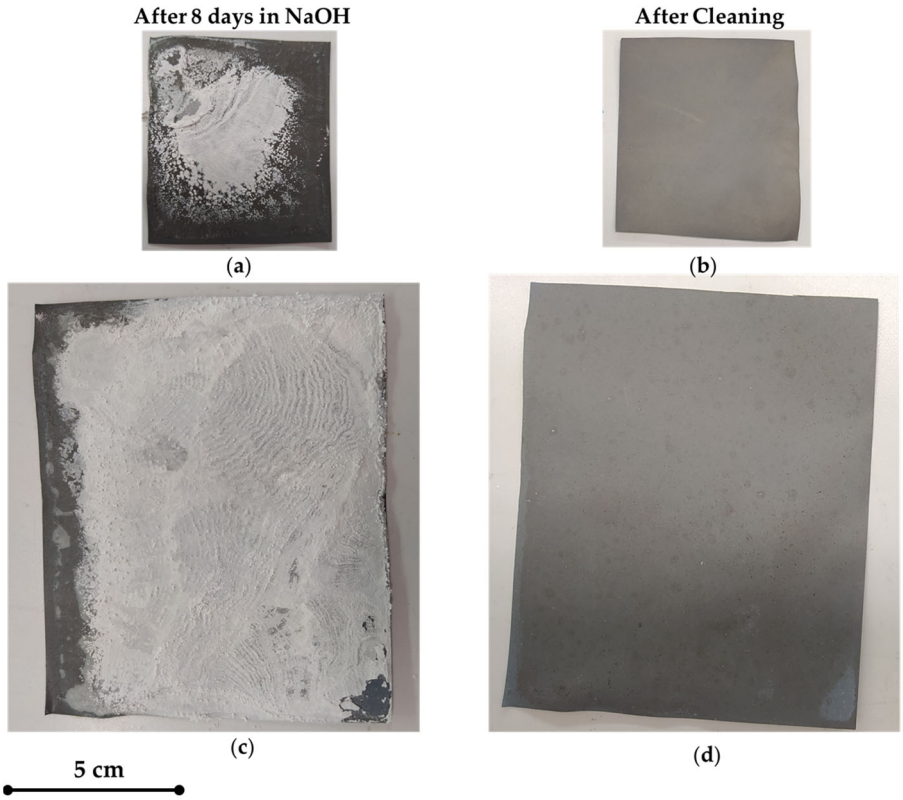

Figure 4. Pictures of the R sample after 8 days in NaOH (**a**) and after cleaning (**b**), and of the C sample after 8 days in NaOH (**c**) and after cleaning (**d**).

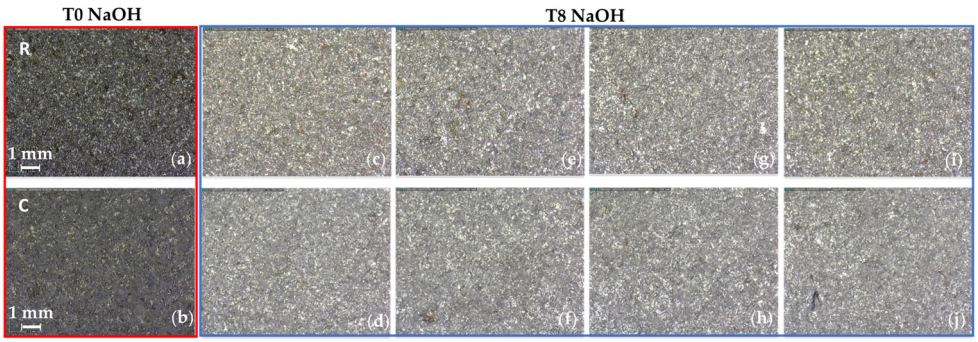

Figure 5. Microscopic image of the R sample (**a**) before and (**b**–**e**) after 8 days in NaOH and of the coated sample C (**f**) before and (**g**–**j**) after 8 days in the same solution.

The effect of the surface corrosion is well evident in the SEM images of the R sample (Figure 6), where the surface initially smooth (Figure 6a) becomes wrinkled after the immersion in NaOH (Figure 6b), and especially after the immersion in NaCl (Figure 6c), where ripples, cracks, and holes large some micrometers appear. The roughness of the surface increases consequently by 0.7% after immersion in NaOH and 24% after immersion in NaCl (Figure 7). In the SEM images of C samples, some cracks are visible in the sponge-like morphology of the coating before starting the immersion tests. In spite of the presence of these cracks, the appearance of the coating does not change drastically after the immersion in NaOH and NaCl solutions (Figure 8b–d). It emerges that after immersion in NaOH (Figure 8b), the ripples seem slightly to increase, whereas after the

immersion in NaCl, the coating seems to lose its characteristic sponge-like morphology in some limited areas (Figure 8c); in others, crystalline structures appear, maybe as salt residual (Figure 8d). Accordingly, the surface roughness increases by 1% and decreases by −3% after the immersion in NaOH and NaCl, respectively (Figure 7).

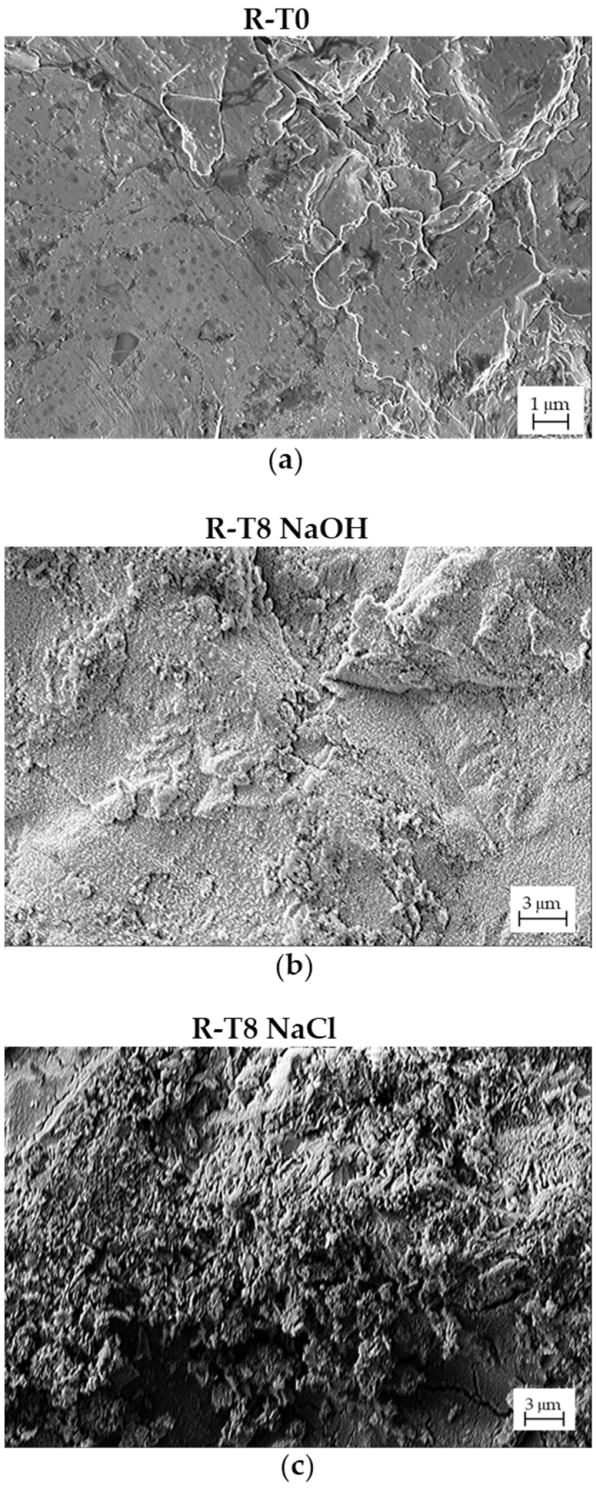

Figure 6. SEM images of the R sample (**a**) before and (**b**,**c**) after 8 days in NaOH and NaCl.

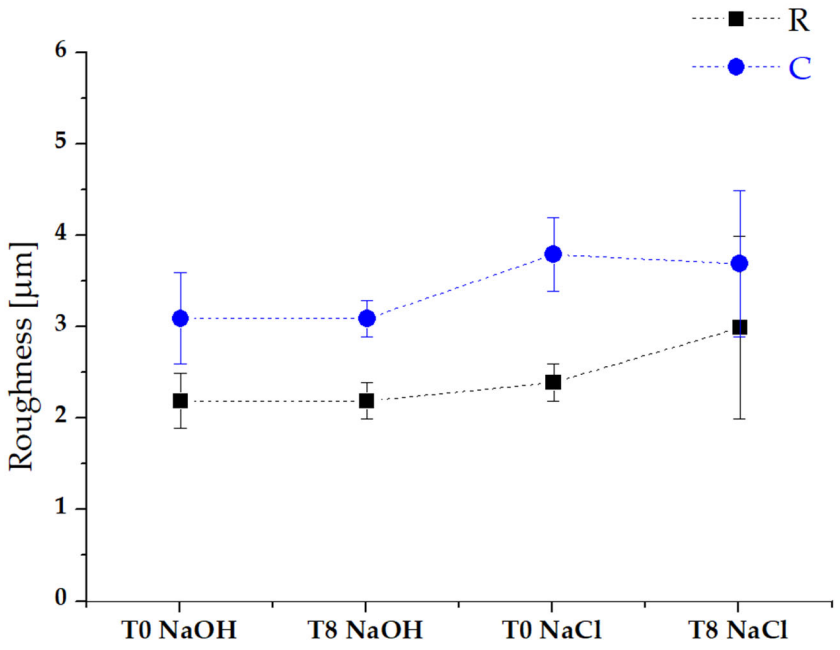

Figure 7. Roughness Ra measured at T = 0 and after 8 days of immersion in NaOH or NaCl. The dark squares and blue circles indicate the Ra values for the reference and the coating samples, respectively.

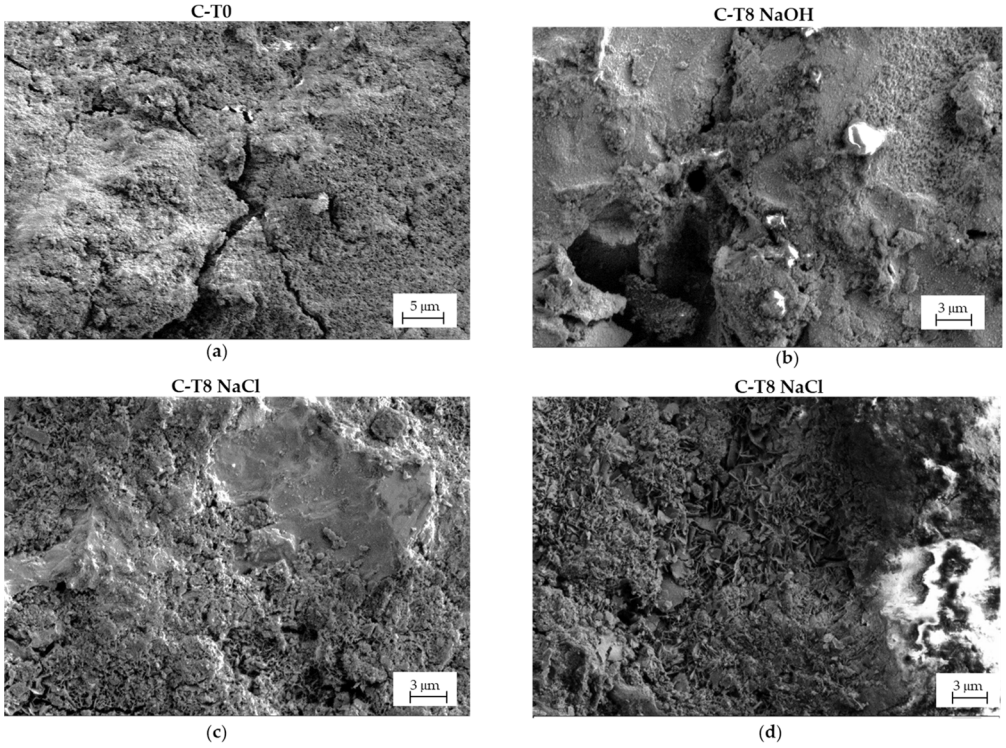

Figure 8. SEM images of the C sample (**a**) before and (**b**–**d**) after 8 days in NaOH and NaCl.

The chemical composition of the R and C samples' surfaces before and after immersion in NaOH and NaCl was determined by EDX. In Table 1, the wt.% of Fe and O are reported, along with the percentage variation with respect to the T0.

Table 1. Fe and O composition of the R and C samples surface before and after immersion in NaOH and NaCl, wt.%. The percentage variations with respect to T0 are also reported.

	R-T0	R-T8 NaOH	R-T8 NaCl	C-T0	C-T8 NaOH	C-T8 NaCl
Fe (%)	97.6 ± 2.8	90.9 ± 1.4	79.5 ± 6.2	0 ± 0	2.2 ± 0.2	4.7 ± 2.2
Δ Fe (%)	0	−7	19	0	2	5
O (%)	1.8 ± 0.5	7.4 ± 1.2	20.5 ± 6.1	44.3 ± 1.4	45.7 ± 2.0	46.6 ± 4.5
Δ O (%)	0	311	1039	0	3	5

The R samples exhibit a notable increase in the oxygen component after immersion, indicating the occurrence of a corrosion process, particularly in the case of the saline solution, where the oxygen percentage is over 10 times higher than in the reference. The coated sample, on the other hand, displays a less pronounced level of oxidation. However, it is worth noting that, following exposure to the solution, a certain percentage of iron becomes evident, which was previously entirely absent. This observation suggests a corrosion of the protective coating, causing the underlying material to become exposed. Furthermore, in the case of immersion in NaCl, it was observed that the percentages of Fe and O exhibit a non-negligible dispersion, which can be attributed to the non-uniformity of the corrosion process.

The increase in Fe and O content, ascribed to Fe present in its trivalent or divalent oxidation states [41], leads to an increase in the SFE and WA of R and C samples (Figures 9 and 10), except for the R sample after 8 days in NaOH solution. As a consequence of the oxidation process, the SFE polar component γ_S^P in R samples increases (SP in Table 2), whereas it remains equal to zero for C samples.

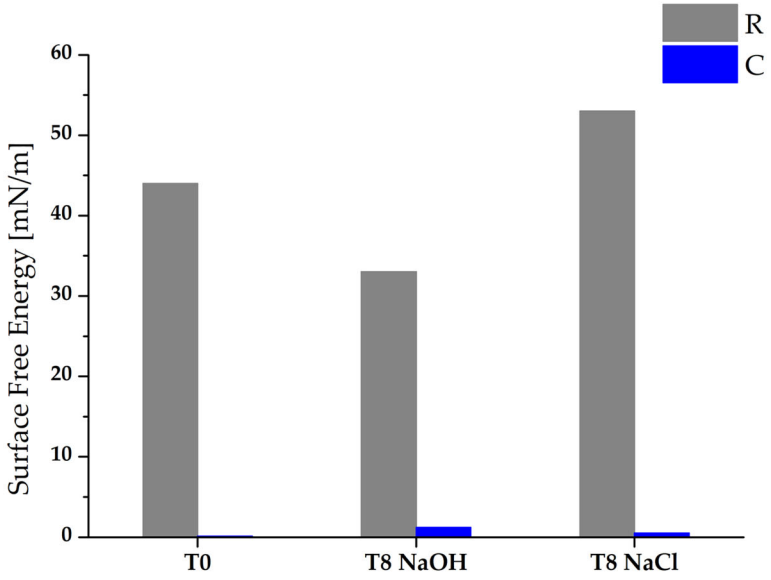

Figure 9. Surface Free Energy (SFE) at T = 0 and after 8-day immersion in NaOH and in NaCl.

In Figure 11, the water contact angle (WCA) of the R and C samples are reported at T0 and after 8 days in NaOH and NaCl after the sample has been cleaned and dried. The R samples also keep their wettability after immersion in solutions. The decrease in WCA after 8 days in NaCl remains within the margin of error, which is significant due to the non-uniform corroded surface. Similarly, the C samples preserve their superhydrophobicity, showing an excellent resistance of the coating to immersion in both solutions.

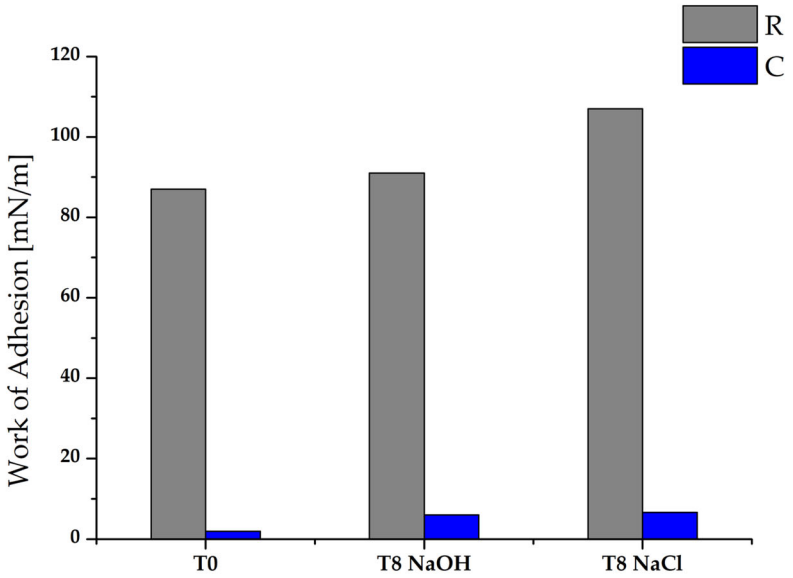

Figure 10. Work of Adhesion (WA) at T = 0 and after 8-day immersion in NaOH and in NaCl.

Table 2. SFE dispersive (γ_S^D) and polar (γ_S^P) components, and Surface Polarity (SP) of R and C samples before and after immersion in NaOH and NaCl.

	R-T0	R-T8 NaOH	R-T8 NaCl	C-T0	C-T8 NaOH	C-T8 NaCl
γ_S^D**(mN/m)**	42.2	24.6	45.7	0.1	1.2	0.5
γ_S^P**(mN/m)**	2.2	8.7	7.6	0.0	0.0	0.0
SP (%)	4.9	26.1	14.3	0.0	0.0	0.0

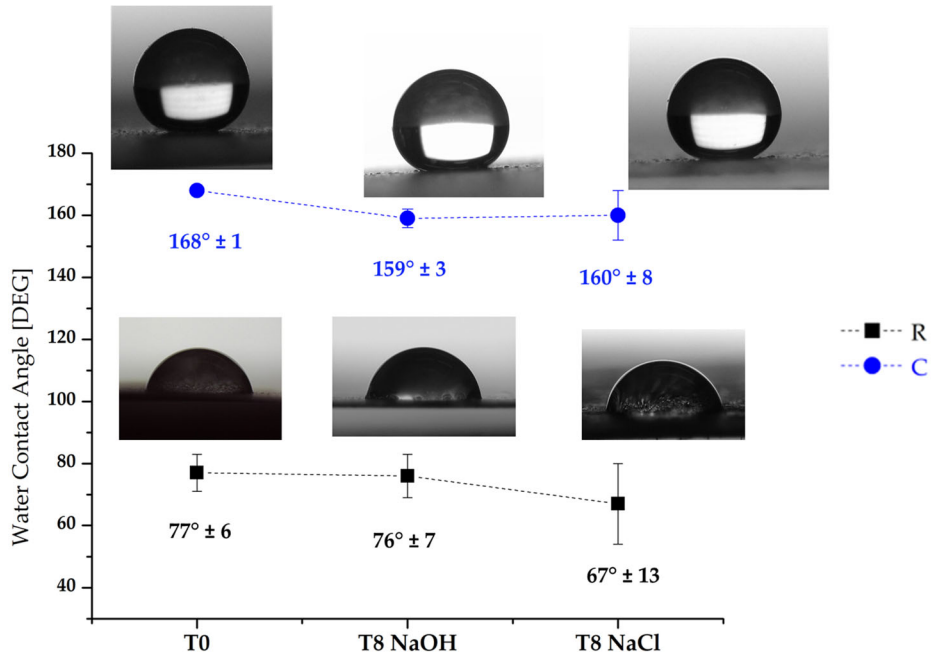

Figure 11. Water contact angle (WCA) at T = 0 and after 8-day immersion in NaOH or NaCl. The dark squares and blue circles indicate the WCA values for the reference R and the coating C samples, respectively. Pictures of the water droplets taken during the acquisitions are reported.

4. Conclusions

In this study, we explored the corrosion resistance of stainless-steel samples coated with superhydrophobic material after exposure to NaCl and NaOH solutions, yielding significant insights. While the superhydrophobic coating did not completely eliminate corrosion, it notably reduced its extent, particularly in the challenging NaCl environment. In both liquid environments, the application of the coating resulted in reduced formation of ripples and surface roughness, decreased iron oxide formation due to oxidative processes, and a lower value of the Surface Free Energy. Importantly, the surface retained its superhydrophobic properties even after an 8-day immersion in NaCl and NaOH solutions. This underscores the coating's promise in preserving surface properties and minimizing corrosion, making it a valuable solution for protecting stainless-steel components in practical applications. Indeed, keeping in mind the application of the exploited coating as a passive Ice Protection System mostly for aeronautical applications, future work will be focused on the feasibility of implementing this technique in actual aircraft components and real-world conditions, including the degradation of coatings under electromagnetic radiation, such as UV light exposure, testing varying humidity levels, considering factors such as maintenance requirements, durability, and cost-effectiveness.

5. Patents

Data reported in this manuscript refer to coatings whose formulation is protected by the patent submission: F. Piscitelli, Italian Patent Application N. IT102021000032444, "Rivestimento superidrofobico e ghiacciofobico di un substrato, metodo per il suo ottenimento e substrato così rivestito", 23 December 2021, and F. Piscitelli, F. Substrate superhydrophobic and icephobic coating, method for obtaining it and substrate thus coated, International Patent Application N° PCT/IB2022/062672, 22 December 2022.

Author Contributions: Conceptualization, F.P. and A.V.; methodology, F.P.; validation, F.P.; formal analysis, F.P.; investigation, F.P. and A.V.; resources, F.P.; data curation, F.P. and A.V.; writing—review and editing, F.P. and A.V. All authors have read and agreed to the published version of the manuscript.

Funding: This research was funded by the Italian Ministry for University and Research (MUR) through the National Aerospace Research Program (PRORA) D.I. n° 662/2020 as TECH-ICE project.

Data Availability Statement: Data are contained within the article.

Acknowledgments: A.V. would like to thank Felice Alberto Sfregola for his support in the acquisition of SEM images.

Conflicts of Interest: The authors declare no conflict of interest.

References

1. Li, L.; Chakik, M.; Prakash, R. A Review of Corrosion in Aircraft Structures and Graphene-Based Sensors for Advanced Corrosion Monitoring. *Sensors* **2021**, *21*, 2908. [CrossRef] [PubMed]
2. Cole, G.K.; Clark, G.; Sharp, P.K. *The Implications of Corrosion with Respect to Aircraft Structural Integrity*; DSTO Aeronautical and Maritime Research Laboratory: Melbourne, VIC, Australia, 1997.
3. Czaban, M. Aircraft Corrosion—Review of Corrosion Processes and Its Effects in Selected Cases. *Fatigue Aircr. Struct.* **2018**, *2018*, 5–20. [CrossRef]
4. Parveez, B.; Kittur, M.I.; Badruddin, I.A.; Kamangar, S.; Hussien, M.; Umarfarooq, M.A. Scientific Advancements in Composite Materials for Aircraft Applications: A Review. *Polymers* **2022**, *14*, 7. [CrossRef] [PubMed]
5. Bi, P.; Li, H.; Zhao, G.; Ran, M.; Cao, L.; Guo, H.; Xue, Y. Robust Super-Hydrophobic Coating Prepared by Electrochemical Surface Engineering for Corrosion Protection. *Coatings* **2019**, *9*, 452. [CrossRef]
6. Mohamed, A.M.A.; Abdullah, A.M.; Younan, N.A. Corrosion Behavior of Superhydrophobic Surfaces: A Review. *Arab. J. Chem.* **2015**, *8*, 749–765. [CrossRef]
7. Zhao, Z.; Luo, G.; Cheng, M.; Song, L. Water-Repellent Coatings on Corrosion Resistance by Femtosecond Laser Processing. *Coatings* **2022**, *12*, 1736. [CrossRef]
8. Erbil, H.Y. Practical Applications of Superhydrophobic Materials and Coatings: Problems and Perspectives. *Langmuir* **2020**, *36*, 2493–2509. [CrossRef]

9. Liu, J.; Fang, X.; Zhu, C.; Xing, X.; Cui, G.; Li, Z. Fabrication of Superhydrophobic Coatings for Corrosion Protection by Electrodeposition: A Comprehensive Review. *Colloids Surf. A Physicochem. Eng. Asp.* **2020**, *607*, 125498. [CrossRef]
10. Piscitelli, F.; De Palo, R.; Volpe, A. Enhancing Coating Adhesion on Fibre-Reinforced Composite by Femtosecond Laser Texturing. *Coatings* **2023**, *13*, 928. [CrossRef]
11. Bai, Y.; Zhang, H.; Shao, Y.; Zhang, H.; Zhu, J. Recent Progresses of Superhydrophobic Coatings in Different Application Fields: An Overview. *Coatings* **2021**, *11*, 116. [CrossRef]
12. Vazirinasab, E.; Jafari, R.; Momen, G. Application of Superhydrophobic Coatings as a Corrosion Barrier: A Review. *Surf. Coat. Technol.* **2018**, *341*, 40–56. [CrossRef]
13. Manoj, A.; Ramachandran, R.; Menezes, P.L. Self-Healing and Superhydrophobic Coatings for Corrosion Inhibition and Protection. *Int. J. Adv. Manuf. Technol.* **2020**, *106*, 2119–2131. [CrossRef]
14. De Palo, R.; Emanuele Mazzarone, A.; Volpe, A.; Gaudiuso, C.; Paolo Mezzapesa, F.; Spagnolo, V.; Ancona, A. Investigation of Laser-Induced Surface Structures (LIPSS) on Quartz and Evaluation of Their Influence on Material Wettability. *Opt. Laser Technol.* **2024**, *169*, 110097. [CrossRef]
15. Zhang, L.; Zhou, A.G.; Sun, B.R.; Chen, K.S.; Yu, H.Z. Functional and Versatile Superhydrophobic Coatings via Stoichiometric Silanization. *Nat. Commun.* **2021**, *12*, 982. [CrossRef] [PubMed]
16. Wang, D.; Sun, Q.; Hokkanen, M.J.; Zhang, C.; Lin, F.Y.; Liu, Q.; Zhu, S.P.; Zhou, T.; Chang, Q.; He, B.; et al. Design of Robust Superhydrophobic Surfaces. *Nature* **2020**, *582*, 55–59. [CrossRef] [PubMed]
17. Jung, T.; Choi, H.; Kim, J. Effects of the air layer of an idealized superhydrophobic surface on the slip length and skin-friction drag. *J. Fluid Mech.* **2016**, *790*, R1. [CrossRef]
18. Chen, S.; Chen, Y.; Lei, Y.; Yin, Y. Novel Strategy in Enhancing Stability and Corrosion Resistance for Hydrophobic Functional Films on Copper Surfaces. *Electrochem. Commun.* **2009**, *11*, 1675–1679. [CrossRef]
19. Zhao, L.; Liu, Q.; Gao, R.; Wang, J.; Yang, W.; Liu, L. One-Step Method for the Fabrication of Superhydrophobic Surface on Magnesium Alloy and Its Corrosion Protection, Antifouling Performance. *Corros. Sci.* **2014**, *80*, 177–183. [CrossRef]
20. Rao, A.V.; Latthe, S.S.; Mahadik, S.A.; Kappenstein, C. Mechanically Stable and Corrosion Resistant Superhydrophobic Sol-Gel Coatings on Copper Substrate. *Appl. Surf. Sci.* **2011**, *257*, 5772–5776. [CrossRef]
21. Xiang, T.; Han, Y.; Guo, Z.; Wang, R.; Zheng, S.; Li, S.; Li, C.; Dai, X. Fabrication of Inherent Anticorrosion Superhydrophobic Surfaces on Metals. *ACS Sustain. Chem. Eng.* **2018**, *6*, 5598–5606. [CrossRef]
22. Li, L.; Zhang, Y.; Lei, J.; He, J.; Lv, R.; Li, N.; Pan, F. A Facile Approach to Fabricate Superhydrophobic Zn Surface and Its Effect on Corrosion Resistance. *Corros. Sci.* **2014**, *85*, 174–182. [CrossRef]
23. Wu, L.K.; Zhang, X.F.; Hu, J.M. Corrosion Protection of Mild Steel by One-Step Electrodeposition of Superhydrophobic Silica Film. *Corros. Sci.* **2014**, *85*, 482–487. [CrossRef]
24. Liu, Y.; Li, S.; Zhang, J.; Liu, J.; Han, Z.; Ren, L. Corrosion Inhibition of Biomimetic Super-Hydrophobic Electrodeposition Coatings on Copper Substrate. *Corros. Sci.* **2015**, *94*, 190–196. [CrossRef]
25. Zhang, F.; Chen, S.; Dong, L.; Lei, Y.; Liu, T.; Yin, Y. Preparation of Superhydrophobic Films on Titanium as Effective Corrosion Barriers. *Appl. Surf. Sci.* **2011**, *257*, 2587–2591. [CrossRef]
26. Delimi, A.; Galopin, E.; Coffinier, Y.; Pisarek, M.; Boukherroub, R.; Talhi, B.; Szunerits, S. Investigation of the Corrosion Behavior of Carbon Steel Coated with Fluoropolymer Thin Films. *Surf. Coat. Technol.* **2011**, *205*, 4011–4017. [CrossRef]
27. Piscitelli, F. Rivestimento Superidrofobico e Ghiacciofobico Di Un Substrato, Metodo per Il Suo Ottenimento e Substrato Così Rivestito. Patent IT102021000032444, 23 December 2021.
28. Piscitelli, F. Substrate Superhydrophobic and Icephobic Coating, Method for Obtaining It and Substrate Thus Coated. Patent PCT/IB2022/062672, 22 December 2022.
29. Piscitelli, F.; Tescione, F.; Mazzola, L.; Bruno, G.; Lavorgna, M. On a Simplified Method to Produce Hydrophobic Coatings for Aeronautical Applications. *Appl. Surf. Sci.* **2019**, *472*, 71–81. [CrossRef]
30. *G31-72(1999)*; Standard Practice for Laboratory Immersion Corrosion Testing of Metals. ASTM International: West Conshohocken, PA, USA, 2004.
31. Kumar, R.; Vinjamuri, B.; Kumar, V.R.D.; Prakash Rao, C.R.; Bharat, V. Corrosion Behavior of Cenosphere Reinforced Al7075 Metal Matrix Composite-An Experimental Approach. *J. Miner. Mater. Charact. Eng.* **2018**, *6*, 424–437. [CrossRef]
32. Sojoudi, H.; Wang, M.; Boscher, N.D.; McKinley, G.H.; Gleason, K.K. Durable and Scalable Icephobic Surfaces: Similarities and Distinctions from Superhydrophobic Surfaces. *Soft Matter.* **2016**, *12*, 1938–1963. [CrossRef]
33. *ISO 4288:1996*; Geometrical Product Specifications (GPS)—Surface Texture: Profile Method—Rules and Procedures for the Assessment of Surface Texture. International Organization for Standardization ISO: Geneva, Switzerland, 1996.
34. *ASTM D7490-13*; Standard Test Method for Measurement of the Surface Tension of Solid Coatings, Substrates and Pigments Using Contact Angle Measurements. American Society for Testing and Materials: West Conshohocken, PA, USA, 2013.
35. Owens, D.K.; Wendt, R.C. Estimation of the Surface Free Energy of Polymers. *J. Appl. Polym. Sci.* **1969**, *13*, 1741–1747. [CrossRef]
36. Żenkiewicz, M. Methods for the Calculation of Surface Free Energy of Solids. *J. Achiev. Mater. Manuf. Eng.* **2007**, *24*, 137–145.
37. Piscitelli, F.; Chiariello, A.; Dabkowski, D.; Corraro, G.; Marra, F.; Di Palma, L. Superhydrophobic Coatings as Anti-Icing Systems for Small Aircraft. *Aerospace* **2020**, *7*, 2. [CrossRef]
38. Houska, C. *Deicing Salt-Recognizing The Corrosion Threat*; TMR Consulting: Pittsburgh, PA, USA, 2007.

39. Pickering, H.W.; Frankenthal, R.P. On the Mechanism of Localized Corrosion of Iron and Stainless Steel. *J. Electrochem. Soc.* **1972**, *119*, 1297. [CrossRef]
40. Zou, J.-Y.; Chin, D.-T. Mechanism of Steel Corrosion in Concentrated NaOH Solutions. *Electrochim. Acta* **1987**, *32*, 1751–1756. [CrossRef]
41. Hedberg, Y.; Karlsson, M.E.; Blomberg, E.; Odnevall Wallinder, I.; Hedberg, J. Correlation between Surface Physicochemical Properties and the Release of Iron from Stainless Steel AISI 304 in Biological Media. *Colloids Surf. B Biointerfaces* **2014**, *122*, 216–222. [CrossRef]